

# Discovery and Study of Nearby Habitable Planets with Mesolensing

Rosanne DiStefano & Christopher Night

*Harvard-Smithsonian Center for Astrophysics, 60 Garden Street, Cambridge, MA 02138*

## ABSTRACT

We demonstrate that gravitational lensing can be used to discover and study planets in the habitable zones of nearby dwarf stars. If appropriate software is developed, a new generation of monitoring programs will automatically conduct a census of nearby planets in the habitable zones of dwarf stars. In addition, individual nearby dwarf stars can produce lensing events at predictable times; careful monitoring of these events can discover any planets located in the zone of habitability. Because lensing can discover planets (1) in face-on orbits, and (2) in orbit around the dimmest stars, lensing techniques will provide complementary information to that gleaned through Doppler and/or transit investigations. The ultimate result will be a comprehensive understanding of the variety of systems with conditions similar to those that gave rise to life on Earth.

### 1. Introduction: Lensing by Planets in the Habitable Zone

Microlensing has been considered as a method best suited to discover distant planets in, e.g., in the Magellanic Clouds, M31, the Galactic Bulge, Halo, and several kiloparsecs from us in the Galactic disk. Recently, it has been pointed out that lensing can provide a way to discover and study nearby (within  $\approx 1$  kpc) planetary systems, providing complementary information to that obtained from Doppler and/or transit studies (Di Stefano 2007). Nearby planets are intriguing because detailed observations are possible. If life exists on other planets, we will find it first and learn most about it on planets within a few hundred parsecs.

The importance of water to Earth life has suggested that we define a zone of habitability around each star to be the region in which liquid water can exist on the surface of a planet that has an atmosphere. The literature suggests that we can express  $a$ , the separation between the central star of mass  $M$ , and a planet in the habitable zone as

$$a = 0.13 \text{ AU } h \left( \frac{M}{0.25 M_{\odot}} \right)^{\frac{3}{2}}, \quad (1)$$

where  $h$  is approximately equal to unity in the middle of the habitable zone, and to  $2/3, 4/3$  at its inner and outer edge, respectively (Charbonneau & Deming 2007; Tarter et al. 2007; Scalo et al. 2007). There is presently significant uncertainty in this equation. The nearby dwarf Gliese 581, with a stellar mass of  $0.31 M_{\odot}$ , has three known planets, one of which has an  $h$  value of 1.39 and is generally considered to be possibly habitable. Another of its planets has an  $h$  value of 0.41, and is generally considered not to be habitable (von Bloh et al. 2007; Selsis et al. 2007), though mitigating effects have been proposed (Chylek & Perez 2007).

The idea motivating our work is to explore the action as a gravitational lens of a nearby dwarf star that hosts a planet in its zone of habitability. The deflection of light from a distant star by an intervening mass causes the image of the source to be split, distorted, and magnified. When the lens is located in our Galaxy, and has mass comparable to that of a star or planet, the images of the source are separated by too small an angle to resolve. We can, however, detect the increase in the amount of light received from the source when its position,  $u$ , projected onto the lens plane is comparable to the Einstein radius,  $R_E$ .

$$R_E = 0.13 \text{ AU} \left[ \left( \frac{M}{0.25 M_{\odot}} \right) \left( \frac{D_L}{10 \text{ pc}} \right) \left( 1 - \frac{D_L}{D_S} \right) \right]^{\frac{1}{2}}, \quad (2)$$

where  $D_L$  is the distance to the lens and  $D_S$  is the distance to the source star. We have assumed that the mass of the planet is a small fraction of the mass of the star. Expressing  $u$  in units of  $R_E$ , the magnification is 34%, 6%, 2%, 1% when  $u = 1, 2, 3, 3.5$ , respectively.

Comparing equations (1) and (2) reveals that the spatial scale that defines the habitable zone is compatible with the size of the Einstein ring for a wide range of stellar masses and distances,  $D_L$ . This is fortuitous, because the chances of detecting a planet around a lens star are greatest when the orbital distance is comparable in size to the Einstein radius.

In this Letter we focus on planetary systems located within about a kiloparsec. These systems are near enough that we can hope to conduct follow-up observations to learn more about the planet and perhaps eventually test for the presence of life. It is convenient to define the parameter  $\alpha$  to be the ratio between the semimajor axis and the value of the Einstein radius:  $a = \alpha R_E$ . Figure 1 shows values of  $\alpha$  as a function of distance, for planets in the zones of habitability around their stars. Depending on the stellar mass, planets in the habitable zone are detectable through their action as lenses for planetary systems as close to us as a parsec (for the lowest-mass dwarf stars), and out to distances as far as a kiloparsec or more when the stellar mass is  $0.5 M_{\odot}$  or larger.

## 2. Signatures of Lensing by Planets in the Habitable Zone

### 2.1. Orbital Motion

Signatures of the lensing by a planetary system have been studied theoretically (Mao & Paczynski 1991; Gould & Loeb 1992; Di Stefano & Scalzo 1999a,b; Griest & Safizadeh 1998). Four planets have been observed (Bond et al. 2004; Udalski et al. 2005; Gould et al. 2006). These discoveries were made by searching for a signature in which an ongoing event caused by a star’s action as a lens is punctuated by a short-lived light curve feature caused by the presence of a planet.

In many cases, nearby planets in the habitable zone will produce signatures that are similar to those already observed for more distant systems. Figure 1 shows, however, that the ratio between the event duration (usually one to three times the Einstein diameter crossing time,  $\tau_E$ ) and orbital period can be close to or even greater than unity for these systems. This can produce new types of events, increase the overall event rate, and decrease some event durations. Figure 2 illustrates the region of deviation whose geometry and rotation produce detectable events.

We have conducted a set of simulations for each of a sequence of nearby systems with planets in the zone of habitability. The systems we worked with are marked by a cross in Figure 1; the stellar mass is  $0.25 M_\odot$ , the orbital separation is 0.1AU, and the systems differ from each other only in their distance from us, which ranges from 10 pc to 200 pc. We have computed the rate of deviations, for each of several levels of detectability. To demonstrate that rotation is an important factor for these systems, we have run the simulation twice: once taking rotation into account and once assuming no rotation. (See Table 1.) Typical examples of the deviations produced by our simulation are shown in Figure 3.

### 2.2. Detectability

Several trends are evident in Table 1. Naturally, in all cases, the greater the sensitivity to deviations, either shorter in duration or smaller in strength, the larger the rate. In all cases, caustic crossings are negligible. Generally, the farther that  $\alpha$  is from the so-called critical zone around  $\alpha = 1$ , the fewer the deviations. The effect is allayed in many circumstances, however, by rotation. For  $\Delta = 0.003$  and 0.01, we still see a very appreciable rate of one-hour events even down to  $\alpha = 0.223$ . Because rotation significantly enhances detectability, it is important to take its contribution into account.

It must be noted that our simulation assumes that the size of the source star’s disk is

infinitesimal, an assumption that is justified in many but not all situations for nearby lenses. Generally, if the timescale of the deviation  $t_{dev}$  is much greater than the time it takes the lens to traverse the source’s disk, finite source size effects can be neglected. This holds when:

$$t_{dev} \gg 0.04 \text{ hr} \left( \frac{R_*}{R_\odot} \right) \left( \frac{50 \text{ km/s}}{v} \right) \left( \frac{D_L}{100 \text{ pc}} \right) \left( \frac{10 \text{ kpc}}{D_S} \right) \quad (3)$$

### 3. Expected Event Rate

#### 3.1. Targeting a Single Dwarf Star for Lensing Studies

Unlike other methods of planet detection, gravitational lensing relies on light from a more distant star. It is therefore important to ask what fraction of nearby dwarfs will pass in front of bright sources and so can be studied with lensing. Within 50 pc, there are approximately 2 dwarf stars, primarily M dwarfs, per square degree. Consider a star with  $M = 0.3 M_\odot$ , located at 50 pc. For this star,  $\theta_E = R_E/D_L = 0.006''$ , and, if its transverse velocity,  $v$ , is  $50 \text{ km s}^{-1}$ , it traverses  $0.21'' \text{ yr}^{-1}$ . If the path of a more distant source star must cross within  $\theta_E$  of the lens in order for there to be a detectable event, the lens can generate one event per (year, decade, century) if the density of the source field (per sq. arcsecond) is (16, 5.0, 1.6). An accurate calculation of the rate of detectable events must consider that, when we monitor dense source fields, even the smallest resolution element,  $\theta_{mon}$  is likely to contain more than one star. In order for the magnification of a particular source star to be detectable, the increase in the amount of light we receive from it must be enough to produce a certain fractional change,  $f_T$ , in the amount of light received from a region  $\theta_{mon} \times \theta_{mon}$ . The rate at which a single star generates detectable events (Di Stefano 2005) is

$$\mathcal{R}_1 = \frac{0.027}{\text{yr}} \left( \frac{0.1}{f_T} \right) \left( \frac{1''}{\theta_{mon}} \right)^2 \left( \frac{v}{50 \text{ km/s}} \right) \left( \frac{M}{0.3 M_\odot} \right)^{\frac{1}{2}} \left( \frac{50 \text{ pc}}{D_L} \right)^{\frac{3}{2}}. \quad (4)$$

This rate is high enough that, given a dense background field and a known nearby M dwarf in front of it, we can plan observations to detect the action of the dwarf as a lens. For example, if the photometry can be sensitive enough to allow  $f_T = 0.01$ , and if the angular resolution is good enough to allow  $\theta_{mon} = 0.5''$ , the rate of detectable events can be comparable to one per year, higher if  $f_T$  can be made smaller. Because it is possible for the rate per lens to be so large, we call nearby lenses “high-probability lenses” or *mesolenses*

(Di Stefano 2005).<sup>1</sup>

This suggests that, by studying the backgrounds behind dwarf stars, we can predict the times of future events and plan frequent, sensitive, high-resolution observations to test for evidence of the planet’s effect as a lens (Di Stefano 2005). What can we learn from targeted observations? We can determine if there is a planet in the habitable zone: we will either discover evidence of it, or place a quantifiable limit on the existence of one. If there is a planet, we can, under ideal circumstances, measure its mass and its projected distance from the star. To plan such observations, we must identify a large reservoir of potential lenses lying in front of dense backgrounds. In front of the Magellanic Clouds, e.g., we expect there to be approximately 200 (1600) dwarf stars with  $D_L < 50$  pc ( $D_L < 200$  pc). Equation (4) indicates that, if observations with small values of  $f_T$  and/or  $\theta_{mon}$  can be conducted, roughly 10% of these stars will produce detectable events within a decade. The first step, therefore, is to study the backgrounds behind the known dwarf stars lying in front of the chosen background field, to determine which are the ones most likely to produce events in the near future, and to predict the likely event times so that appropriate monitoring observations can be planned for the duration of the predicted event. For dwarf stars that do not lie in front of dense fields, serendipitous events are nevertheless possible; one such event has been observed (Gaudi et al. 2007; Fukui et al. 2007). Cross-correlation between the positions of nearby dwarf stars and the positions of more distant sources of light may identify future positional coincidences that can be predicted with high accuracy (Salim & Gould 2000).

### 3.2. Monitoring Studies

Targeted lensing observations have been suggested by a variety of authors (Feibelman 1986; Paczynski 1995; Salim & Gould 2000; Di Stefano 2005), but have not yet been carried out. Instead, astronomers have conducted large observing programs in which they have monitored tens of millions of stars per night (Alcock et al. 2000; Udalski et al. 2000; Derue et al. 2001). More than 3,500 microlensing event candidates have been discovered to date. The microlenses tend to be located at distances greater than several kiloparsecs, and their presence is revealed through their action as lenses. While theoretical work has explored the discovery of nearby lenses by these programs (Di Stefano 2007), several examples of nearby lenses suggest that dwarf stars constitute as many as 10 – 20% of the lenses producing de-

---

<sup>1</sup>The prefix “meso” refers to the fact that both spatial and temporal signatures can be important for nearby lenses. In cosmological applications of lensing, spatial signatures can be important, while microlensing is studied in the time domain.

tectable events (Nguyen et al. 2004; Kallivayalil et al. 2006; Gaudi et al. 2007; Fukui et al. 2007). For monitoring programs, the expected rate of events caused by nearby dwarfs, with constant spatial density  $N_L$ , in front of a source field of area  $\Omega$ , is

$$\mathcal{R}_{tot} = \frac{0.069}{\text{yr}} \left( \frac{\Omega}{\text{sq. deg.}} \right) \left( \frac{0.1}{f_T} \right) \left( \frac{1''}{\theta_{mon}} \right)^2 \left( \frac{N_L}{0.1 \text{ pc}^{-3}} \right) \left( \frac{v}{50 \text{ km/s}} \right) \left( \frac{M}{0.3 M_\odot} \right)^{\frac{1}{2}} \left( \frac{D_L}{50 \text{ pc}} \right)^{\frac{3}{2}}. \quad (5)$$

This implies that events must have already been detected by ongoing monitoring programs, such as OGLE, which has  $f_T$  and  $\theta_{mon}$  roughly equal to 0.1 and  $1''$ , respectively. OGLE monitors almost 100 sq. degrees in the Galactic Bulge, but not all at the same cadence. Considering just 50 sq. degrees, OGLE data must include 3.4 events per year caused by dwarf stars within 50 pc, and perhaps as many as 38 per year caused by dwarf stars within 250 pc. Within the next year, a sensitive all-sky monitoring program, Pan-STARRS will begin monitoring the sky from Hawaii; approximately 5 years after that, LSST will begin even more sensitive and frequent observations from Chile. If values of  $f_T = 0.02$ , and  $\theta_{mon} = 0.5''$  can be achieved over 200 sq. degrees (including dense background fields and serendipitous positions of background stars behind foreground dwarfs), then these programs will detect events caused by 270 (3000) dwarf stars within 50 pc (250 pc). Each of these events provides an opportunity to test for the presence of a planet in the zone of habitability.

For monitoring programs, it is worthwhile to consider which signal will provide a trigger to let us know that a planet-lens event is occurring. For the now-standard case of microlensing planet detection, the signature of the planet is a deviation of an ongoing event from the point-lens light-curve shape. As Figure 3 shows, this can also happen for planets in the habitable zone when the underlying event has a large value of  $A_{max}$ , i.e., when the source track passes close to the star. In many cases, however, the value of  $A_{max}$  is small. It is therefore important to note that, whether the value of  $A_{max}$  is large or small, the presence of the dwarf star is itself an important signature. When any deviation is detected, and when there is a dwarf star along the line of sight, frequent sensitive monitoring is called for. Such monitoring will either discover evidence of a planet, or will place limits on the existence of one.

#### 4. Conclusion

Until now, searches for habitable planets have relied on very successful techniques based on Doppler shifts and on transits. We point out that gravitational lensing is a potentially powerful complement to these proven methods. Because it relies on light from background sources, gravitational lensing can discover planets in the habitable zones of even the dimmest

stars, and can be successful even if spectral lines and/or the measured flux exhibit erratic variations. Because it relies only on the distribution of the lens-system’s mass, even face-on systems, inaccessible to Doppler and transit techniques, can be studied.

The challenge faced by lensing studies is that the lens must pass in front of a background source of light. This requires that the planetary system lie in front of a dense source field, or else that its path happens to bring its projected position close to a background field star. Predictions (Di Stefano 2005), bolstered by the discovery of events caused by nearby lenses (Nguyen et al. 2004; Kallivayalil et al. 2006), indicate that both types of events are common.

Monitoring observations of the present and near future, including OGLE, Pan-STARRS, and LSST can discover events caused by planets in habitable zones of nearby stars. In most cases, the presence of the star and its proper motion will already have been catalogued by the same monitoring data. Software must be developed to recognize even subtle lensing-like deviations in real time, so that when they occur at the location of a known possible lens, a separate program of frequent follow-up observations can be initiated.

Targeted lensing observations are a new frontier. As has been the case for Doppler and transit studies, it will take time for them to yield results, but the results are well worth it. For any given nearby dwarf star, we can discover the presence of a planet, or place limits on the existence of one. If a planet is discovered, the quantities that can be derived under ideal circumstances are the planet’s mass, its separation from the star, and its orbital period.

The authors are grateful to Charles Alcock, David Charbonneau, Matthew Holman, Penny Sackett, Dimitar Sasselov for conversations. This work was supported in part by AST-0708924.

## REFERENCES

- Alcock, C., et al. 2000, *ApJ*, 542, 281
- Bond, I. A., et al. 2004, *ApJ*, 606, L155
- Charbonneau, D. & Deming, D. 2007, *ArXiv e-prints*, 706
- Chylek, P. & Perez, M. R. 2007, *ArXiv e-prints*, 709
- Derue, F., et al. 2001, *A&A*, 373, 126
- Di Stefano, R. 2005, *ArXiv Astrophysics e-prints*

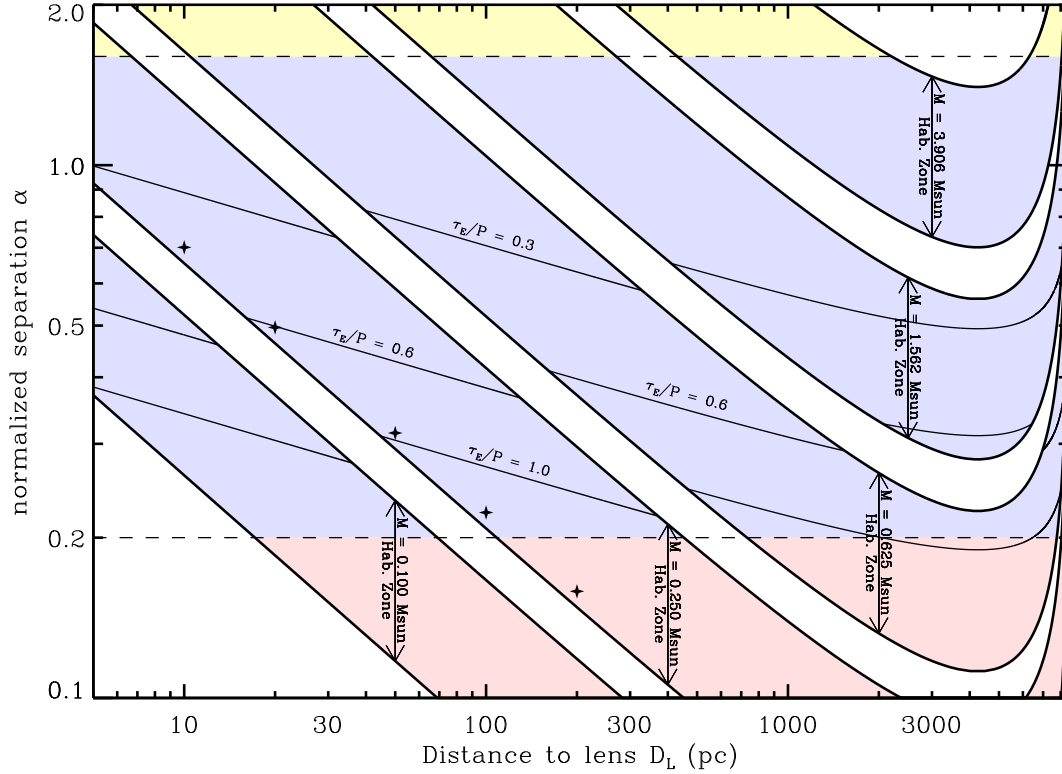


Fig. 1.—  $\alpha$  vs  $D_L$  for the habitable zone of low-mass stars. Each colored bar represents a star with a given mass:  $M = 0.1 M_\odot$  on the lower left, increasing by a factor of 2.5 for each subsequent bar. The lower (upper) part of each bar corresponds to the inner (outer) edge of the habitable zone for a star of that mass. The upper horizontal dashed line at  $\alpha = 1.6$  marks the approximate boundary between “wide” systems, in which the planet and star act as independent lenses (Di Stefano & Scalzo 1999a,b), and “close” systems in which distinctive non-linear effects, such as caustic crossings provide evidence of the planet (Mao & Paczynski 1991; Gould & Loeb 1992). All of the planets detected so far have model fits with  $\alpha$  lying between 0.7 and 1.6. In this range, the effects of caustics are the most pronounced. As  $\alpha$  decreases, the effect of the planet on the lensing light curve becomes more difficult to discern; the horizontal dashed line at  $\alpha = 0.2$  is an estimate of a lower limit. The probability of detecting the planet in such close systems ( $\alpha \leq 0.5$ ) is increased by the orbital motion.



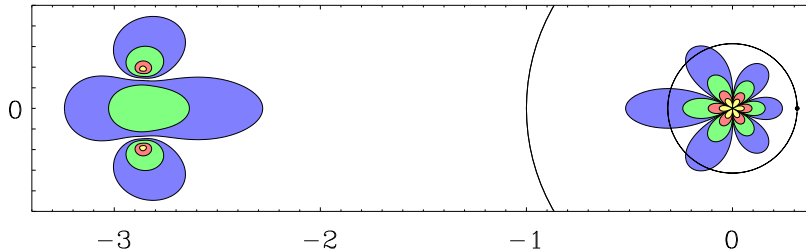


Fig. 2.— Regions in the lens plane that correspond to deviations from the point-lens signature. All distances are measured in units of the Einstein radius. This lens has  $M_{planet}/M = 0.001$  and separation  $\alpha = 0.314$ . If the star is 50pc away and has a mass of  $0.25 M_{\odot}$ , the planet would be in the habitable zone, at an orbital distance of 0.1 AU. The center of mass is placed at the origin, and the star is very slightly offset from this. The inner circle shows the planet’s orbit. At the instant of time depicted, the planet is located to the right of the star. The outer circle shows the Einstein radius; if the source passes through this circle, the peak magnification of the event will exceed 1.34. When the source is within a colored region, the difference  $\Delta$  between the actual magnification and the expected point-lens magnification exceeds a certain amount. Blue (outermost):  $\Delta > 0.1\%$ . Green:  $\Delta > 0.3\%$ . Red:  $\Delta > 1\%$ . Yellow (innermost):  $\Delta > 3\%$ . Note that the sizes of all of these regions are much larger than the caustic structures, which are too small to be shown on this plot. The regions of deviation rotate around the center of mass as the planet orbits. Since the outer region is much farther from the center, it moves much faster than the planet does. This effect increases the probability that the source will pass through a region in which  $\Delta$  is detectable.

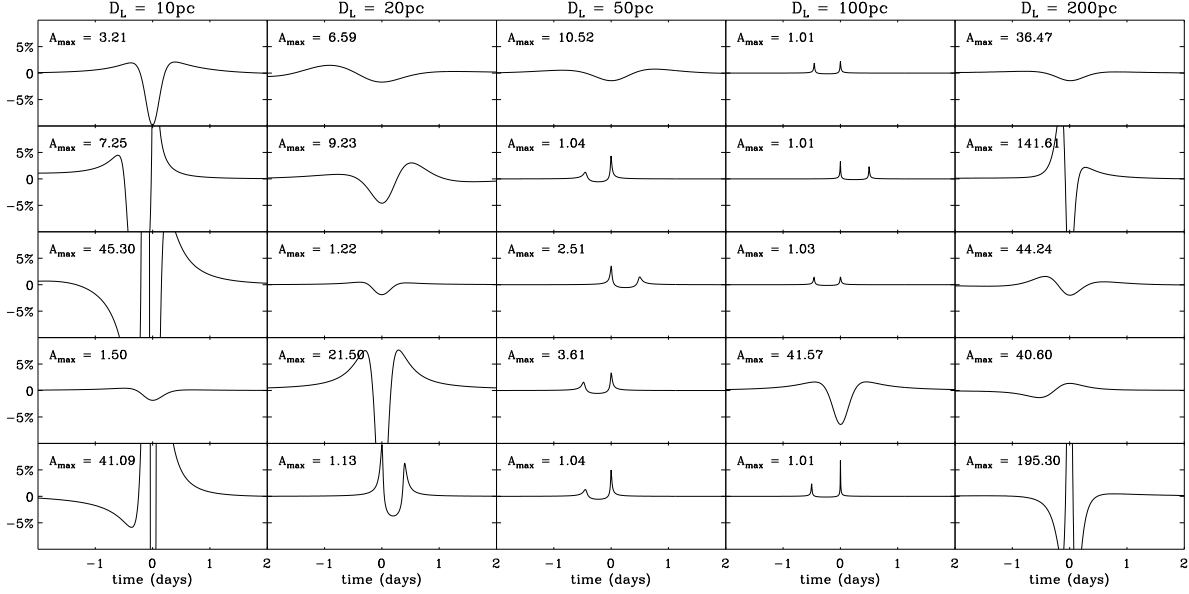


Fig. 3.— Typical deviations from the point-lens form, as found with our simulation. Plotted in each panel is the residual magnification  $\Delta(t)$  due to the planet.  $\Delta(t)$  is the magnification of the source star with respect to time, minus the point-lens amplification that would occur if the planet were not present. The x-axis shows time from the maximum of the deviation in days. For each of the five systems considered in our simulation, five deviations are shown, chosen randomly from the set of events with a deviation of  $\Delta > 0.01$  lasting at least 6 hours. Deviations include a mixture of close approaches (for which  $A_{\max}$  is large) and distant approaches (for which  $A_{\max}$  is small). This is because when  $\alpha$  is small, there are two general regions of deviation in the lens plane: one near to the lens and one far from it, as shown in Figure 2. Deviations on near approaches are due to crossing the region near the lens, and deviations on far approaches are due to crossing the region far from the lens. As  $\alpha$  approaches 1 (i.e., for small  $D_L$ ), these two regions coalesce, and so for  $D_L$  small, there are not two distinct deviation types, but rather a continuum. For the smallest values of  $\alpha$  (i.e., the largest values of  $D_L$ , for a given lens mass), deviations experienced in the outer region tend to be short-lived, so that the longest deviations occur when the source track traverses the central region.

- . 2007, ArXiv e-prints, 712
- Di Stefano, R. & Scalzo, R. A. 1999a, ApJ, 512, 564
- . 1999b, ApJ, 512, 579
- Feibelman, W. A. 1986, PASP, 98, 1199
- Fukui, A., et al. 2007, ApJ, 670, 423
- Gaudi, B. S., et al. 2007, ArXiv Astrophysics e-prints
- Gould, A. & Loeb, A. 1992, ApJ, 396, 104
- Gould, A., et al. 2006, ApJ, 644, L37
- Griest, K. & Safizadeh, N. 1998, ApJ, 500, 37
- Kallivayalil, N., et al. 2006, ApJ, 652, L97
- Mao, S. & Paczynski, B. 1991, ApJ, 374, L37
- Nguyen, H. T., et al. 2004, ApJS, 154, 266
- Paczynski, B. 1995, Acta Astronomica, 45, 345
- Salim, S. & Gould, A. 2000, ApJ, 539, 241
- Scalo, J., et al. Astrobiology, 7, 85
- Selsis, F., et al. 2007, ArXiv e-prints, 710
- Tarter, J. C., et al. 2007, Astrobiology, 7, 30
- Udalski, A., et al. 2005, ApJ, 628, L109
- Udalski, A., et al. 2000, Acta Astronomica, 50, 1
- von Bloh, W., et al. 2007, ArXiv e-prints, 705

| $D_L$ | $\alpha$ | $\tau_E/P$ | $\Delta = 0.003$ |       |       |          | $\Delta = 0.01$ |       |       |          | $\Delta = 0.03$ |       |       |          | $R_{cc}$ |
|-------|----------|------------|------------------|-------|-------|----------|-----------------|-------|-------|----------|-----------------|-------|-------|----------|----------|
|       |          |            | $R_0$            | $R_1$ | $R_6$ | $R_{24}$ | $R_0$           | $R_1$ | $R_6$ | $R_{24}$ | $R_0$           | $R_1$ | $R_6$ | $R_{24}$ |          |
| 10    | 0.701    | 0.428      | 0.80             | 0.79  | 0.78  | 0.64     | 0.58            | 0.59  | 0.57  | 0.44     | 0.45            | 0.45  | 0.42  | 0.15     | 0.01     |
| 10    | 0.701    | 0.428      | 0.68             | 0.68  | 0.68  | 0.64     | 0.52            | 0.51  | 0.51  | 0.44     | 0.41            | 0.41  | 0.40  | 0.22     | 0.01     |
| 20    | 0.496    | 0.604      | 1.48             | 1.50  | 1.48  | 0.96     | 0.90            | 0.89  | 0.79  | 0.22     | 0.37            | 0.37  | 0.29  | 0.04     | 0.001    |
| 20    | 0.496    | 0.604      | 0.80             | 0.80  | 0.80  | 0.77     | 0.43            | 0.43  | 0.42  | 0.32     | 0.23            | 0.23  | 0.21  | 0.07     | 0.001    |
| 50    | 0.314    | 0.954      | 1.50             | 1.52  | 1.13  | 0.20     | 0.56            | 0.52  | 0.09  | 0.06     | 0.29            | 0.21  | 0.05  | 0.01     | 0.000    |
| 50    | 0.314    | 0.954      | 0.40             | 0.40  | 0.40  | 0.36     | 0.16            | 0.17  | 0.16  | 0.06     | 0.08            | 0.09  | 0.07  | 0.01     | 0.000    |
| 100   | 0.223    | 1.345      | 1.03             | 1.00  | 0.12  | 0.08     | 0.52            | 0.30  | 0.05  | 0.03     | 0.24            | 0.07  | 0.03  | 0.00     | 0.000    |
| 100   | 0.223    | 1.345      | 0.19             | 0.19  | 0.18  | 0.13     | 0.09            | 0.09  | 0.08  | 0.02     | 0.04            | 0.04  | 0.03  | 0.00     | 0.000    |
| 200   | 0.159    | 1.891      | 0.96             | 0.26  | 0.06  | 0.04     | 0.52            | 0.06  | 0.03  | 0.01     | 0.09            | 0.02  | 0.02  | 0.00     | 0.000    |
| 200   | 0.159    | 1.891      | 0.10             | 0.08  | 0.07  | 0.04     | 0.05            | 0.04  | 0.03  | 0.01     | 0.02            | 0.02  | 0.01  | 0.00     | 0.000    |

Table 1: Rates for deviations of various strengths, as determined by simulation. For  $M = 0.25M_\odot$ ,  $M_{PL} = 0.26M_{Jupiter}$ , and  $a = 0.1AU$  held fixed, a face-on system was placed at five different distances (as shown on Figure 1). For each value of  $D_L$  there are two rows, the top including rotation, and the bottom for (unrealistic) static systems. Rates are normalized to rate of events for which  $A_{max} > 1.34$ . If the number in the table is 1.00, then there will be as many events with deviations at the given level as there are events with a maximum magnification greater than 1.34. The rate of detectable deviations depends on two factors: the size of deviation  $\Delta$  needed for detection, and the duration. For a given  $\Delta$ , we define  $R_k$  to be the rate of deviations lasting at least  $k$  hours. For instance, if deviations must have a strength of 1% and last 6 hours to be detectable, their rate may be found in the  $R_6$  column under  $\Delta = 0.01$ . Although the rotation period is the same ( $P = 23.1$  days) for all systems considered here, each value of  $D_L$  corresponds to a different Einstein radius  $R_E$  and thus a different event duration  $\tau_E$ . Therefore rotation is expected to play a larger role for more distant systems. This affects the event rate by slightly reducing the rate of long-lived deviations, but greatly increasing the rate of short-lived deviations.  $R_0$  is the theoretical maximum rate of deviations, if infinitely fine sampling could be achieved. Values of  $R_0$  were determined not by simulation but by semi-analytic calculation. They should correspond to the maximum possible rate of deviations, but may be slightly lower than  $R_1$  due to rounding errors.